applied sciences

MDPI

Review

The Progress on Lung Computed Tomography Imaging Signs: A Review

Hanguang Xiao †, Yuewei Li *,†, Bin Jiang, Qingling Xia, Yujia Wei and Huanqi Li

School of Artificial Intelligence, Chongqing University of Technology, Chongqing 401135, China
* Correspondence: ywli@2020.cqut.edu.cn
† These authors contributed equally to this work.

Abstract: Lung cancer is the highest-mortality cancer with the largest number of patients in the world. Early screening and diagnosis of lung cancer by CT imaging is of great significance to improve the cure rate of lung cancer. CT signs mean the information of comprehensive manifestations of diseases at different pathological stages and levels. Automatic analysis of CT images outputs the locations and sizes of lesion regions which can help radiologists to make a credible diagnosis and effectively improve the speed and accuracy of clinical diagnosis. In this paper, we first review the domestic and foreign research progress of lung CT signs, summarize a generic structure for expressing the implementation process of existing methods, and systematically describe the signs research based on the traditional machine learning method and deep learning method. Furthermore, we provide a systematic summary and comparative analysis of the existing methods. Finally, we point out the challenges ahead and discuss the directions for improvement of future work, providing reference for scholars in related fields.

Keywords: lung carcinoma; CT imaging signs detection; computer-aided diagnosis (CAD); deep learning; machine learning

Citation: Xiao, H.; Li, Y.; Jiang, B.; Xia, Q.; Wei, Y.; Li, H. The Progress on Lung Computed Tomography Imaging Signs: A Review. *Appl. Sci.* **2022**, *12*, 9367. https://doi.org/10.3390/app12189367

Academic Editors: Jiaqi Li, Božidar Šarler, Haiping Liu and Jian Zhang

Received: 24 August 2022
Accepted: 16 September 2022
Published: 19 September 2022

1. Introduction

As one of the most serious diseases, lung disease threatens human health. According to the GLOBOCAN2021 database [1], lung cancer remains the leading cause of human death, with approximately 17.96 million deaths globally each year, accounting for 18% of total cancer mortality. Previously, the best way to deal with lung cancer was to perform early cancer screening, which may improve the 5-year survival rate of patients by 16–49% with early detection and treatment. Accompanied by improving computed tomography (CT) imaging technology development, CT images have become the most effective and feasible technique to detect lung cancer. Results from the National Cancer Institute's Lung Cancer Screening Trial indicated that CT detected 4–10 times more cases than chest X-rays [2], reducing the mortality rate of lung cancer by 20.3%. Therefore, it is vitally crucial to use CT for early screening and diagnosis of lung disease.

A "sign" in CT lung scans refers to a radiologic feature that implies a specific disease condition. Radiologists diagnose and detect lesions by analyzing their imaging characteristics in CT scans. In clinical practice, these characteristics are called CT imaging signs (CISs), often known as CT features. CISs are particularly significant for the judgment of benign and malignant pulmonary diseases and the kinds of lesions [3]. Some common CISs can be used as the direct foundation for doctors to diagnose illnesses, while others can aid in restricting the diagnosis. For example, ground-glass opacity (GGO), spiculation, pleural indentation, lobulation, and cavity signs that appear in CT scans are strongly related with malignant lung cancer. However, certain other CISs, such as tree in bud and crescent sign, are connected with benign lung illnesses. Therefore, it provides an essential reference value for the qualitative identification of lung lesions [4,5]. CT imaging signs detection is

more crucial and acts as a basis for the physician to make a credible diagnosis, which can effectively improve the speed and accuracy of clinical diagnosis, and it has great clinical application value.

Due to the diversity of CISs in lung diseases, the current CT image diagnosis process is more dependent on the experience of clinicians, which has that difficulties of strong subjectivity and high misdiagnosis rate. Therefore, adopting computer-aided diagnostic approaches to quantify and reliably diagnose CISs has become an urgent requirement for clinical therapy, which aims to assist clinicians in enhancing the accuracy of diagnosis. However, it is still a challenging task to accurately quantify and detect complex and changeable CISs. To solve these issues, a significant variety of solutions have been presented by local and foreign academics based on distinct processing steps of standard machine learning methods and deep learning methods. In the processing framework based on classic machine learning approaches, researchers have proposed optimization algorithms for lesion segmentation, feature extraction, and false positive reduction. In the study of deep learning approaches, researchers typically create breakthroughs in the design, selection, and matching of network models.

Some progress has been achieved in the investigation of lung CT signs; however, comprehensive assessments of studies from the standpoint of signs are relatively rare. Therefore, this paper first systematically reviews the current research status of lung CT signs, summarizes a general framework to express and describe the existing methods, and makes a systematic analysis and comparison of traditional machine learning methods and deep learning methods in the detection of CISs. Finally, the present obstacles and difficulties to overcome in this field are discussed, and the prospective improvement direction of future study efforts is pointed out.

2. Preliminary

2.1. Lung CT Public Database

The lung medical image database is an essential basis for training and evaluating the detection, classification, segmentation, and retrieval models and algorithms of lung lesions. The existing publicly accessible lung imaging databases are categorized as lesion-oriented, lung disease type-oriented, and sign-oriented, with representative datasets provided in Table 1.

Table 1. Dataset description information.

Dataset	CTScan	Type	Number of Class	Object	Description of the Purpose of Dataset
LIDC-IDRI	1018	DICOM	9	Lesion	Lesion classification and detection.
LUNA16	888	MHD	9	Lesion	Lesion detection algorithm development.
ANEODE09	55	DICOM	4	Lesion	Evaluation of lesion detection algorithms.
ILDs	108	DICOM	13	Lung diseases	Classification of interstitial lung disease.
Lung TIME	157	DICOM	4	Lesion	Lesion classification and detection.
LISS	271	DICOM	9	Sign	CISs classification and detection.

In 2001, the organization of the Lung Image Database Consortium (LIDC) [6] began to build a web-accessible research resource for the development, training, and assessment of CAD approaches for lung lesions. The database was integrated with the Image Database Resource Initiative (IDRI) in 2004, which is a lesion-oriented database. Other lesion-oriented databases include LUNA16 (Lung Nodule Analysis 2016) [7], ANOGE09 (Automatic Nodule Detection) [8], and Lung TIME (Lung Test Images from Motol Environment) [9]. A database for interstitial lung diseases (ILDs) [10] has been developed, which comprises 13 categories such as hypersensitivity pneumonia, pulmonary tuberculosis, pulmonary fibrosis, and interstitial pneumonia. The LISS [11] database is the first public database on CT imaging signs of lung diseases, comprising nine common signs of lung diseases, including lobulation, spiculation, cavity, calcification, pleural indentation, and ground-glass opacity (as illustrated in Figure 1).

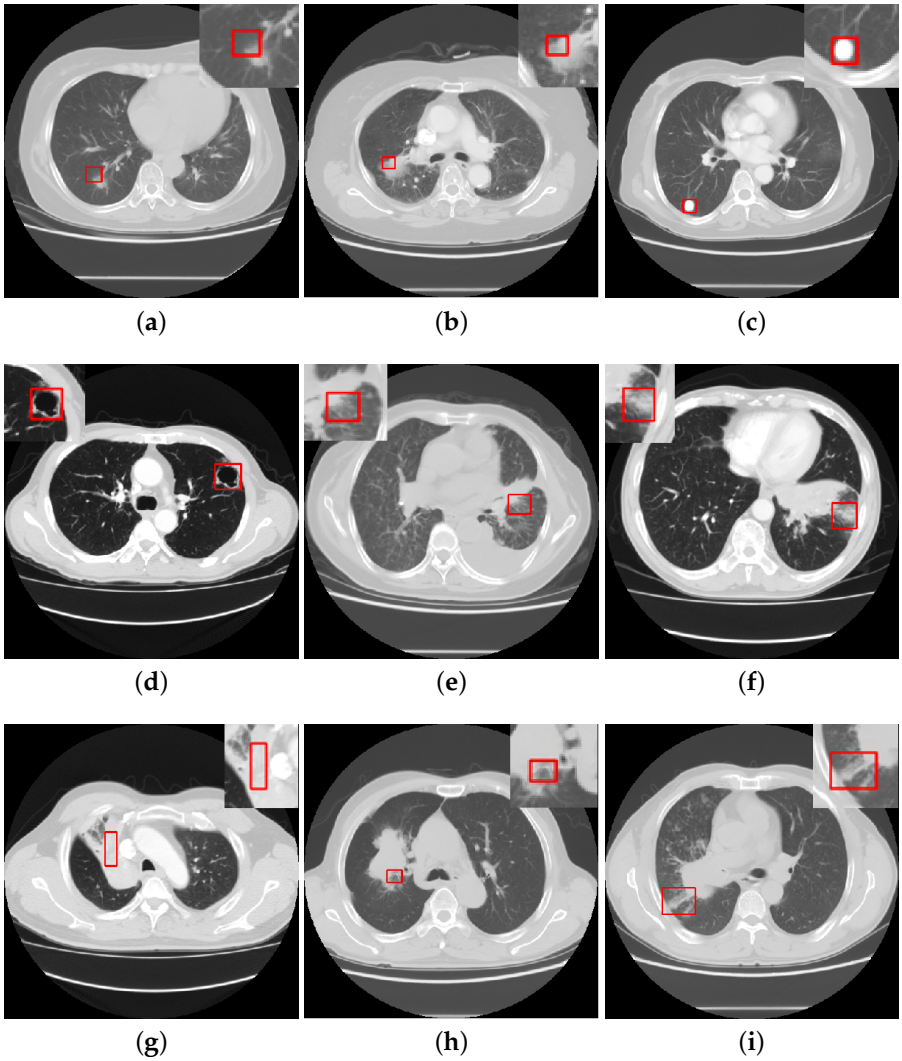

Figure 1. The examples of annotated CISs: (**a**) ground-glass opacity (GGO), (**b**) lobulation, (**c**) calcification, (**d**) cavity and vaculus, (**e**) spiculation, (**f**) obstructive pneumonia, (**g**) bronchial mucus plugs, (**h**) air bronchogram, (**i**) pleural indentation.

2.2. Evaluation Criteria

In order to evaluate the efficiency of the given approach, indices such as sensitivity, specificity, and accuracy are typically utilized in the literature for evaluation. For the reader's convenience, this section highlights the assessment indicators typically applied in the literature, as discussed in detail in Table 2.

Table 2. Evaluation indicators.

Indicator	Definition	Description
Sensitivity	$SE = \frac{TP}{TP+FP}$	True positive rate.
Specificity	$SP = \frac{TN}{TN+FP}$	True negative rate.
Accuracy	$ACC = \frac{TP+TN}{TP+TN+FP+FN}$	Proportion of correct sample to total sample.
Precision	$P = \frac{TP}{TP+FP}$	Proportion of true positive sample to all positive samples.
F1-score	$F1 = \frac{2PR}{P+R}$	Harmonic mean.
ROC	TPR versus FPR curve	$TPR = \frac{TP}{TP+FN}$, $FPR = \frac{FP}{TN+FP}$.
AUC	Total area under the ROC curve	area under curve (AUC).

Note: TP is a true positive; TN is a true negative; FP is a false positive; FN is a false negative.

2.3. The Overview Framework for Detection of CISs

Currently, there are mainly standard multistep detection frameworks and innovative deep learning detection frameworks used to lung CT sign identification. The traditional multistep framework is built on machine learning, which essentially involves four fundamental steps: preprocessing, candidate region segmentation, feature extraction, and false positive reduction. The future stages depend on the preceding step, and the outcomes of each phase will have a considerable effect on the ultimate detection result. The advantage of this framework is that the stages are straightforward to describe and reasonably easy to implement. The disadvantages are that each phase is isolated from the others, the parameters cannot be shared and optimized simultaneously during the training process, and the traditional approaches are limited due to manual feature extraction lacking expression capacity and poor generalization ability.

The innovative deep learning detection framework is based on deep learning. The advantage of this framework is that deep learning methods can automatically extract deep features of an image and perform end-to-end supervised training, making it easier to achieve full automation compared to traditional machine learning methods, and the overall detection performance of the model is better than traditional methods. The disadvantages are equally clear; training deep neural networks needs a considerable quantity of data, and in the medical imaging area, large-scale, well-labeled data resources are limited.

For the reader's simple reference, this paper provides a general detection framework summarizing existing approaches for lung CT sign identification, as illustrated in Figure 2, where the content in the black rectangle box denotes the traditional method and the gray section indicates the deep learning method. CT scans may be preprocessed for further analysis following input to the detection system, and the basic preprocessing methods include eliminating noise from the original CT image for image enhancement and minimizing interference regions for lung parenchyma segmentation, and the system eventually outputs the lesion information.

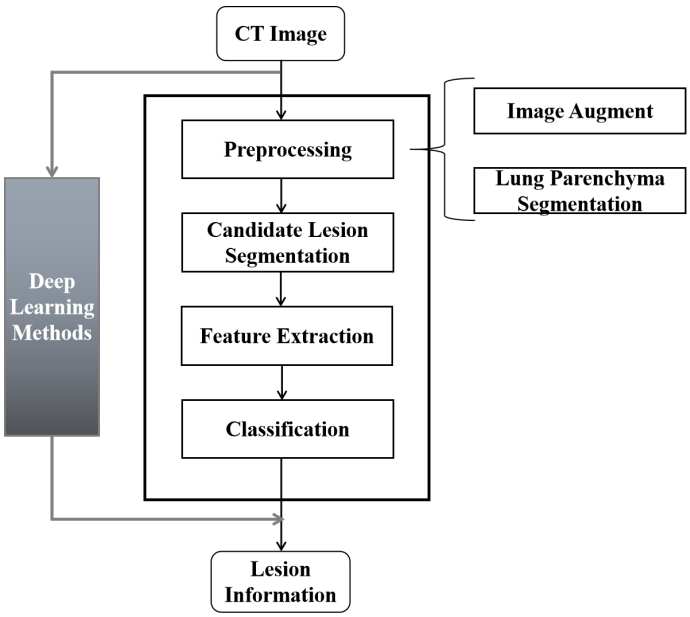

Figure 2. The framework of CISs detection. The traditional multistep framework as shown in the black rectangular box involves four fundamental steps: preprocessing, candidate region segmentation, feature extraction, and false positive reduction. The innovative deep learning detection framework is shown in the gray section.

3. Detection of CISs Based on Traditional Machine Learning Methods

The pulmonary CISs detection method based on standard machine learning may be generally categorized into four main steps: preprocessing, candidate region segmentation,

feature extraction, and feature classification. The image preprocessing approach reduces the noise of the original CT scan by image enhancement and lung parenchyma segmentation, which is an optional step. Previous lung CT scan research has mostly interfered in the processes of potential lesion region segmentation, feature extraction, and feature classification to improve detection performance.

3.1. Candidate Lesion Segmentation

Before identifying the lesion and inputting it for further processing in the process stage, some works will segment the lesion region as a candidate. Candidate lesion region segmentation approaches for lung CIS detection may be split into two categories: threshold methods and mathematical morphological methods.

The main idea of the thresholding method is to select a suitable threshold value to determine the classification of each pixel in the image according to the difference between the CT value of the lesion region and the normal tissue, and to guide the segmentation process to complete the segmentation of the candidate region. Due to the disparity in density of various tissues, a substantial number of false positive regions containing blood vessels will be formed by applying a single threshold to segment lesions. Therefore, researchers generally utilize a multilevel thresholding strategy to segregate potential locations. Guo [12] used K-means clustering to create global thresholds using the L2G (local-to-global multithreshold segmentation) method, and the proposed multithreshold segmentation approach increased the detection performance of GGO signs. Huang [13] proposed an improved adaptive multilevel threshold segmentation approach on the basis of this research, which could identify not only focal GGO but also diffuse GGO and substantially increase the robustness of GGO sign identification. While the multilevel thresholding segmentation algorithm can reduce the false positive rate, the application of the multilevel threshold method will still generate a large number of false positive regions consisting of blood vessels and bronchi when some signs are highly close to the gray values of lung vessels and bronchi.

The morphology approach relies on set theory and mathematical operations, which measure and extract the corresponding shape features according to the structure of images. The essential notion of this approach lies in the selection of structural elements, which may be employed to complete different image analyses and create alternative structures. Dhara [14] proposed a technique based on differential geometry to compute spiculation, lobulation, and spherical signs using segmented nodule masks of diverse morphologies. However, the approach is poorly generalized due to the complexity and diversity of CISs structures and the impossibility to compute numerous indications using a single structural element, and the method is only relevant to images of lesions with considerable variations in gray values at edge locations. In addition, the morphological open–close operation can overcome the problem of a significant number of false positive regions produced by the inability of the threshold approach to correctly split lesions and vessels. Cui [15] used morphological methods to recognize calcification signs, smoothed the boundaries of the obtained candidate areas, applied open operation to select corrosion strength, disconnected narrow areas and eliminated protruding areas, and used close operation to fill the cavity to better segment calcified and noncalcified areas and reduce the generation of false positive areas during lesion segmentation.

The contrast analysis of the threshold method and the mathematical morphology method revealed a comparable amount of research using both types of methods for lung sign segmentation, which is characterized by combining digital image processing methods and machine learning methods for CISs segmentation. Since pulmonary lesions may contain more adherent blood vessels, the threshold approach is more likely to create false positive regions compared to the mathematical morphology method, and its segmentation performance needs to be improved. In addition, the results of this research cannot be compared directly due to variances in the kind and quantity of CISs investigated. However, the general situation demonstrates that the threshold approach is largely applied to the

segmentation of bigger organs, such as lung parenchyma [16], while the mathematical morphology method is mainly applied to the segmentation of lesion regions [17–20].

3.2. Feature Extraction

CT sign recognition approaches based on traditional machine learning methods mainly adopt manual design of features or descriptors. The manually designed features are defined by experts using professional medical knowledge to describe lung tissues and are more commonly used, such as histogram of oriented gradients (HOG), local binary pattern (LBP), local intensity order pattern (LIOP), dense scale-invariant feature transform (SIFT), global context feature, graphics feature, texture feature, wavelet feature, and geometric shape feature.

Due of the diversity of CISs in lung diseases, previous proposed feature extraction approaches incorporated various aspects to characterize the area of interest. In 2012, Song [21] combined the visual word bags of HOG and LBP to depict the suspected lesion locations in lung CT images for sign classification and identification, and they conducted five-fold cross-validation on the LISS dataset with an average recognition accuracy of 98.8%. This approach confirms that combining HOG and LBP characteristics for sign identification is superior to employing individual HOG (95.7%) or LBP (90.4%) features. In view of the efficiency of this technique, some researchers adapted this notion to the field of image retrieval and achieved the retrieval of nine frequent indicators of lung diseases with good performance [22,23].

Although fusing numerous features can increase the performance of the model to a certain amount, it is unnecessary to blindly add features, which may not improve the performance of the model much and will cause a waste of computational resources. In 2014, Liu [24] added CT value histogram (CVH) characteristics on the basis of [21]. However, the identification accuracy was only 80.26% and the specificity was just 70.22%. Therefore, the key to enhancing the performance of the model is to analyze the association between the characteristics and to adopt various features in an informed manner.

A comparison of the above methods reveals that whether using a single feature or fusing multiple features, the above methods mainly extract low-level semantic features such as shape and grayscale, which are not able to describe the key information of a large number of sophisticated clinical images, and thus cannot meet the requirements of high accuracy, a variety of sign recognition, and classification in clinical applications.

3.3. Feature Classification

During the candidate region segmentation and feature extraction, the research object should be extracted as much as feasible, regardless of the amount of false positives created. After feature extraction for all candidate regions segmented, a classification method needs to be implemented to separate the true lesion regions from the fake ones, which entails conducting false positive elimination. For the detection of lung CT signs, researchers usually adopt the feature classifier method; that is, they calculate the image features of the discernible target region and false positive region from the candidate region, carry out feature selection, and the candidate regions are classified using a discriminative classification model or combinatorial classifier.

While blindly adding features is not effective in improving model performance, based on the hypothesis that different types of features may contain complementary information, researchers have conducted a lot of research on how to select suitable features to achieve better classification performance, and have proposed different feature selection algorithms. Sun [25] and Liu [24] refined the traditional genetic optimization feature selection algorithm to improve the classification performance of benign and malignant lung nodules by selecting the optimal subset of features for identifying CISs from the numerous graphical feature sets of lung nodules. Ma [26] proposed a feature selection method based on minimum spanning trees, which considered the relationship between different features on the basis of the traditional method and captured the relationship between the discriminative power

of different features, so as to select the most important features for sign recognition. The feature selection technique was tested on 511 actual CT images with a classification accuracy of 91.96%. This approach is a significant advance in feature selection methods, breaking away from the traditional genetic algorithms, and provides a new route for research into improved feature selection algorithms.

In the classification stage, the choice of classification algorithm plays a crucial role in the recognition result. Common classifiers include support vector machine (SVM), decision tree (DT), Bayesian classifiers, K-nearest neighbor (KNN), linear discriminant classifier, etc. Although tremendous progress has been achieved in the performance of traditional single classifiers, the performance of single classifiers in practical applications is still unsatisfactory. Since the fusion of many features may compensate for the lack of a single feature, the application of fusing multiple classifiers to compensate for the limitations of a single classifier in classification seems to be a promising approach.

Current classification fusion work may be classified into two groups: soft classification fusion and hard classification fusion. The core of these soft classification fusion approaches is accomplished by weighing the outputs of each classifier and assigning each classifier a weight (between 0 and 1). The weight is defined by the training performance of the classifier on the data, and the output of the classifier is the weighted result of the predicted probability of different classifiers on the category to make the final judgment. The key of this strategy lies in how to assign weights to the classifiers. Liu [27] merged matrix and classification confidence value to calculate the weight assigned to each classifier, and completely analyzed the previous performance of the classifier for data training and the features of the present data. The classification accuracy achieved 76.79%, which may greatly enhance the classification performance of signs compared to a single classifier (SVM: 72.02%, KNN: 70.94%, DT: 68.38%).

The hard classification fusion method is implemented by a voting mechanism, where the classifier outputs a classification label, with 1 indicating a recognized class and 0 indicating the other class, and counts the number of all classifiers for each class and selects the highest number of votes as the final class. Ref. [26] trained k AdaBoost classifiers to recognize nine common indicators, such as spiculation, cavity, pleural indentation, and lobulation, acquired k classification decisions, and ultimately utilized voting to achieve the final decision. This strategy enhanced the classification accuracy by 15.17% compared to the soft classification method [27]. Compared to the fusion methods based on soft and hard classification, the weighting of classifiers in soft classification is influenced by more factors and is difficult to define, while the hard classification method is able to combine the results of each classifier, which avoids errors caused by misclassification of a single classifier, and is also easier to implement, making this method more widely used.

With the continual development of algorithms for candidate region segmentation, feature extraction, and feature classifier, the model performances of lung CT CIS detection approaches based on traditional machine learning have demonstrated a rising trend. However, as these three steps are independent of each other, the outcomes of the previous step will immediately impact the following step, making it difficult to adjust the parameters of each step concurrently to produce improved detection results after model training. Moreover, with the development trend of big data in medical imaging, traditional machine learning algorithms do not show enough satisfactory performance for solving big data problems and cannot meet the requirements of high accuracy and a variety of sign recognition and classification in clinical applications.

4. Detection of CISs Based on Deep Learning Methods

Compared with detection methods based on traditional machine learning, the advantage of this framework is that deep learning methods can automatically extract deeper features of the image and perform end-to-end supervised training, making it easier to achieve full automation compared to traditional machine learning methods, and the overall detection performance of the model is better than traditional methods. The disadvantage is

also evident that training deep neural networks takes a considerable quantity of data, while in the field of medical images, the large-scale and well-labeled data resources are limited.

This section elaborates on the application of deep learning methods in lung CT scanning and discusses deep learning methods in classification and image retrieval. The network structure utilized in the literature is visualized in Figure 3.

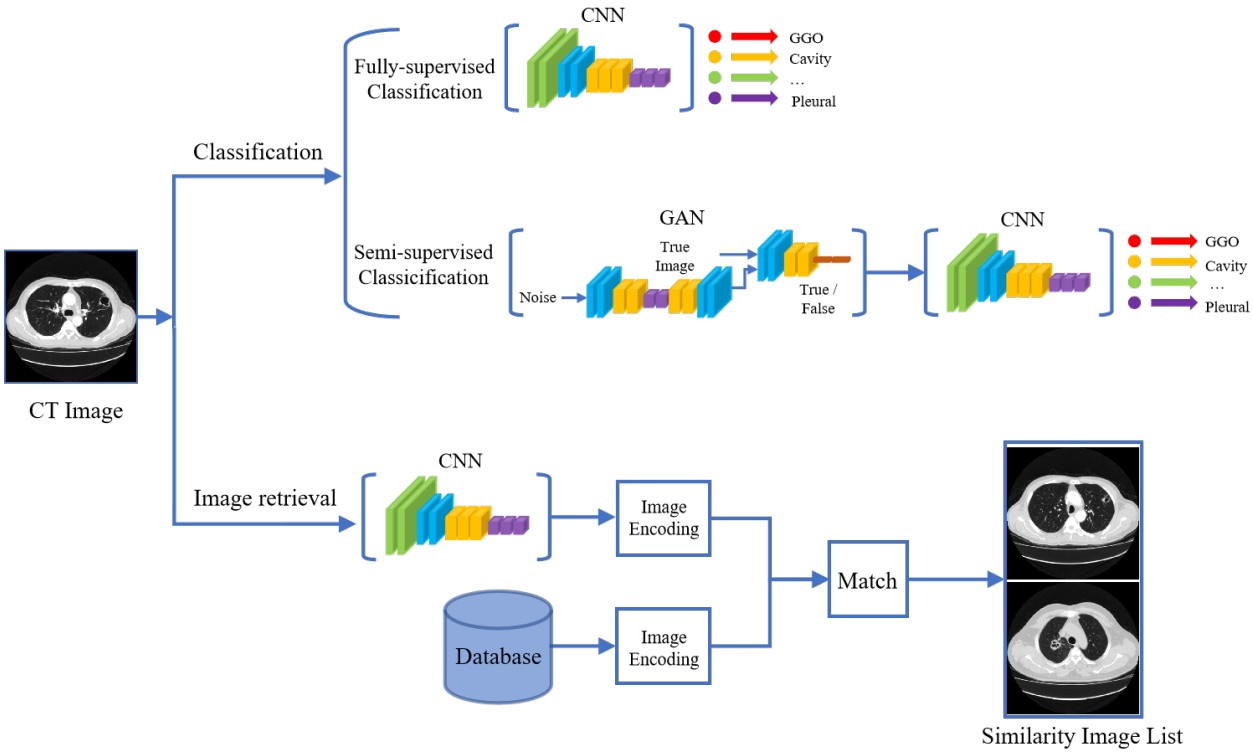

Figure 3. Network frameworks used in deep learning methods: Fully-supervised classification sends the CT images to the convolutional neural network (CNN) for classification and outputs different CISs class; while semi-supervised classification addresses the problem of lack of dataset by using the generative adversarial network (GAN) to generate a large number of high-quality samples to expand the training data and then send them to the convolutional neural network for classification; image retrieval sends the images to the convolutional neural network to extract features and calculate the similarity between these features and the features of the image to be retrieved to return a collection of lesion images similar to the query image.

4.1. Classification

4.1.1. Fully-Supervised Classification

CNN is the major approach of deep learning applied to lung CT CIS detection. The network comprises a convolutional layer, a pooling layer, and a fully connected layer. The shallow network comprises a convolutional layer and a pooling layer to extract the region of interest, whereas the deep network consists mostly of a fully connected layer to accomplish tasks such as logistic regression and classification. The strategy of using CNN is divided into two parts: off-the-shelf CNN and fine-tuning. Off-the-shelf CNN refers to the use of CNN models trained in other domains as feature extractors without retraining CNN models using medical images, and employing CNN features as supplemental information to existing manual features. Fine-tuning refers to pretraining CNN models on natural image datasets (COCO, ImageNet) and then conducting supervised model refining on medical image datasets.

The training of CNN models requires a vast quantity of data. However, in the field of medical image processing, the premise of having a sufficient amount of well-labeled data for training may not hold, and direct training of models from scratch is prone to overfitting. Therefore, previous works employ off-the-shelf CNN; that is, the traditional characteristics

of current medical imaging data are merged with the features extracted by CNN to identify signs. In 2019, Han [28] employed CifarNet as a CNN feature extractor, trained on the Cifar-10 dataset and then transferred to the cavity samples for fine-tuning, to identify cavity signs by merging CNN features with classical HOG and LBP features. Their work compared the classification impacts of CNN, HOG, LBP, and fused features, and the FS score was 0.0757, 0.1136, 0.1138, and 0.1472, respectively. Results demonstrate that the HOG and LBP features give extra relevant information, and that a fusion features model can outperform that of using any single feature. Furthermore, our technique greatly enhances the sensitivity (85% vs. 70% vs. 62%) of recognizing cavity signs compared to existing advanced cavity sign identification systems [29,30]. The proposed feature fusion approach indicates that knowledge learned from various datasets rather than the training sample may provide an effective solution to the problem of limited well-labeled medical images.

Due to the huge variances in different datasets, fusion features may not be able to accurately reflect the characteristics of the target field. Therefore, a natural idea is to fine-tune the obtained CNN model using the target field data to improve detection accuracy. Han [31] employed GGO samples to retrain the acquired CifarNet and trained multiple CNN models based on multiple-receptive-field, and then fine-tuned and merged multiple CNN models. The model fusion sensitivity reached 96.64%, which was considerably better than the classification performance of Shin [32] (70%) and Song [33] (83%) after fine-tuning only a single CNN model. In [34], the Inception model replaced CifarNet and boosted the specificity of the model by 21.74%. While making great progress compared to previous approaches, the quantity of the dataset needed to train a high-capacity deep learning framework is quite large. However, the annotated medical images are frequently expensive to obtain.

4.1.2. Semi-Supervised Learning in Classification

Training deep classification models needs a vast quantity of annotated data. Unlike natural images, annotating medical images is a costly and time-consuming process. To deal with such a problem, the major two strategies are data augmentation [35] and transfer learning [36]. In the traditional data augmentation approach, a number of visual transformations of an image are employed to create images, which can introduce diversity into the training data to some extent and minimize the risks of overfitting of the models. However, the diversity given by visual transformation is still not enough; besides, these transformations influence the distribution of the original dataset and introduce additional noise and offset. Transfer learning needs pretraining on a large-scale natural image dataset and then fine-tuning on the target dataset; however, fine-tuning the CNN model on a restricted dataset can easily lead to overfitting.

To relieve the dependency of manually labeled data, a promising technique named semi-supervised learning (SSL) has attracted increased attention in recent years, which clearly highlights the potential usefulness of employing unlabeled data. Previous lung CT CISs detection approaches based on semi-supervised learning are generally based on GAN [37], which can learn from existing data to produce high-quality pictures, enabling cross-modal data production and image-to-image conversion. He [38] used GAN to create a large number of high-quality CISs samples to expand the training data in order to improve the classification performance of the signs. Unlike transfer learning approaches, the method does not acquire new information from other datasets; the classification model does not need to be retrained and fine-tuned; both the GAN and the CNN are trained on the same dataset; and the distribution of data is consistent. The strategy enhances the accuracy and specificity of the model by 6.7%, 12.8%, 6.6%, and 5.7%, respectively, compared to typical data augmentation [35] and transfer learning methods [36].

While the method described above is an enlightening sign for semi-supervised learning based on sign detection, there are still some issues. The performance of the classification model in the above work is strongly reliant on the quality of the created CISs, and the high-quality CISs samples in this work are generated once and will not be updated. Adding

the generated false positive samples into the subsequent training will introduce severe overfitting, which directly degrades the classification performance. To overcome this issue, Zheng [39] designed an enhanced DCGAN framework based on this GAN to produce simulated samples of unlabeled data. In contrast to the one-off synthesis of samples by He et al., this study continually updates the quality of the created CISs, thereby decreasing the influence of the generated false positive samples on the following classification performance. As the above two methods are for different kinds of signs, the classification results cannot be compared directly, but overall, the above research shows that GAN can provide a promising solution for sign recognition when sign samples are limited; however, the related research has not received sufficient attention, which is worth further exploration by researchers.

4.2. Image Retrieval

With the remarkable success of CNN in the field of medical imaging, the natural question is whether we can apply CNN to the field of image retrieval. The foundation of the sign recognition approach based on image retrieval consists of the three steps of image feature extraction: similarity calculation, feature indexing, and dimensionality reduction. Due to the high dimensionality of the image features derived in the feature extraction stage, vast storage space is needed to preserve the features of images in the retrieval process in the face of massive medical images, which takes a lot of time to retrieve. Therefore, it is required to construct an index of characteristics to ensure efficient access. The hash image retrieval method maps the image features from the high-dimensional space to the low-dimensional binary space through some mapping relationship, and expresses the distance similarity coefficient between the query image and the database image in terms of the Hamming distance between the binary codes. Using hash image retrieval can allow recovery of images quickly and precisely, and may considerably minimize the storage space, which is extensively utilized in the field of medical image retrieval.

Traditional medical image retrieval systems generally extract visual features such as shape, texture, and grayscale from images and then return a collection of lesion images similar to the query image by calculating the similarity between these aspects and the features of the image to be retrieved. The fundamental benefit of image retrieval methods based on deep learning is the integration of CNN with hash coding to increase the performance of image retrieval. In 2017, Zhao [40] used CNN to automatically extract image features, added a hash coding layer on the CNN, and created a deep-learning-based hash network model to accomplish image retrieval based on lung CT signs. Compared to the standard image retrieval method, the retrieval performance was enhanced by 2–5% on average.

In 2021, Zhang [41] used a 3D ResNet network instead of the CNN and optimized the hash codes by the alternative minimization regular optimization approach, enhancing the average impact of the model by 5–8%. The proposed method illustrates that the selection of deep neural networks can increase the performance of image retrieval. In the same year, Yahia [42] proposed the YOLOv4 object detection model to implement the retrieval of lung CT signs, which compressed the retrieval time to 0.1 ms without affecting the retrieval accuracy. This study further established that a deep neural network with better performance plays a significant role in increasing retrieval performance. In addition, the similarity measure between images is also a vital step in determining retrieval performance. In order to retrieve comparable signs more effectively, Ma [43] presented a multilevel similarity measure approach. Different from traditional approaches that only compute visual or semantic similarity, the suggested method is capable of computing level-specific similarity and optimum cross-level complementary similarity. It can attain roughly 80% accuracy and requires only 3.6 ms for the retrieval procedure.

In summary, different deep neural networks combined with different hashing algorithms have distinct implications on retrieval accuracy and efficiency. Determining the ways in which to select effective deep neural networks for feature extraction and how to integrate deep learning with more efficient hashing algorithms to increase retrieval per-

formance remain the focus of future research in the field of image retrieval based on deep learning. Furthermore, the majority of the cited research above focus on the categorization of lung nodules or lung diseases. The recognition or categorization of signs is merely one stage in retrieval, rather than the ultimate aim of the research. More emphasis should be placed on the end-to-end identification or classification of signs.

A comparative analysis of lung CT signs based on deep learning approaches demonstrates that the originality of methods proposed in recent years mostly consists of feature extraction, and the detection performance of models employing fusion features is typically better than that of models using single features. Different feature extraction networks have a direct influence on the classification or detection performance of the model. How to develop an appropriate neural network to extract deep features of images is the emphasis for further study.

5. Discussion

Comparative analyses between different methodologies mentioned in this study are summarized in Table 3. It is worth mentioning that due to the varied characteristics of the sign detection algorithms described in the research, only the performance metrics utilized in most of the literature are mentioned in the table. Some works also obtained good results [14], but they are not shown in the table because alternative metrics are utilized, which are difficult to compare. Through comparison examination of existing methodologies, present approaches for identifying CT signs in the lung disease contain the following basic characteristics:

1. **CISs classification.** Current work is able to obtain above 90% of the classification performance in one or more of the three assessment metrics: sensitivity, specificity, and accuracy. In terms of datasets, earlier work on sign classification mostly depended on the publicly accessible LISS dataset, although there was also some successful research using private data for CISs classification [20,24]. It is not possible to directly compare the classification results because of the differences in datasets and the CISs studied, but the performance of model classification shows an upward trend on the whole, with deep learning methods outperforming traditional machine learning methods for both the classification of single signs and the classification of multiple classes of signs.
2. **CISs segmentation.** Segmentation of lesions is essential to improve the performance of sign classification and detection. The major approaches are the threshold and morphological methods. As lung lesions contain additional blood vessels, the threshold method of segmenting lesions tends to produce a large number of false positive areas and is mainly used for the segmentation of larger organs, such as the lung parenchyma, while the morphological method can effectively remove blood vessels and is mainly applied to the segmentation of small lesion areas.
3. **CISs detection.** While having achieved great progress, most of the present approaches largely focus on CISs classification tasks. There is a lack of research focusing on object detection of CISs. However, people are more interested in lesion detection tasks in medical imaging as opposed to classification tasks, which may be for the following reasons: objection detection networks are much more complex than classification networks and require higher quantity and quality of data. However, there is a wide variety of signs of lung lesions, and as the differences between signs are small, it is very difficult to accurately detect and quantify them.

It is worth mentioning that most of the recent research on the lungs have concentrated on lung nodules or on the benign and malignant classification of lung disease, and much of the material discussed in this article was published two years ago. There is a lack of material focusing on object detection of CISs in recent years.

Table 3. The performance comparison of detection methods for CISs.

Author	Year	Dataset	Sensitivity %	Specificity %	Accuracy %	Others	AUC	Task	Method Type
Guo et al.	2016	LISS	**100**	33.13	-	-	-	GGO segment	Threshold
Huang et al.	2018	LISS	**100**	-	-	-	-	GGO segment	Threshold
Cui et al.	2019	LISS	56.37	**92.29**	89.89	-	-	Calcification segment	Morphology
Song et al.	2015	ILDs	70	-	-	F1-score: 0.80	-	ILDs classification	Deep learning
Shin et al.	2016	ILDs; Others	70	-	-	F1-score: 0.74	-	Lymph node and ILDs classification	Deep learning
Han et al.	2018	LIDC-IDRI	**96.64**	71.43	82.51	F1-score: 0.83	-	GGO classification	Deep learning
Han et al.	2019	LISS; LIDC-IDRI	85	59	59	-	-	Cavity classification	Deep learning
Song et al.	2012	Private	**91.8**	**98.5**	**98**	-	-	Nine CISs classification	Machine learning
Liu et al.	2014	LISS	70.2	**97.2**	80.26	-	-	Nine CISs classification	Machine learning
Liu et al.	2015	Private	70.4	**96.84**	76.79	-	-	Nine CISs classification	Machine learning
Ma et al.	2016	Private	**97.65**	**99.03**	**91.96**	-	-	Nine CISs classification	Machine learning
He et al.	2019	LISS	**92.73**	**99**	**91.83**	-	-	Nine CISs classification	Deep learning
Zheng et al.	2019	LISS; LIDC-IDRI	82.22	**93.17**	88.67	-	-	Five CISs classification	Deep learning
Zheng et al.	2019	LISS; LIDC-IDRI	-	-	-	-	Mean AUC: 0.9184	Five CISs classification	Deep learning
Ma et al.	2017	LISS	-	-	-	mAcc: 77.49%	0.4854	Nine CISs retrieval	Machine learning
Zhao et al.	2017	LISS; LIDC-IDRI	-	-	**93.52**	-	-	Six CISs retrieval	Deep learning
Kashif et al.	2020	LISS	-	-	-	mAcc: 70%	0.58	Nine CISs retrieval	Machine learning
Ma et al.	2020	Private	-	-	80	-	-	Nine CISs retrieval	Machine learning
Zhang et al.	2021	LIDC-IDRI; Private	-	-	**94.83**	-	-	Nine CISs retrieval	Deep learning
Yahia et al.	2021	LISS	-	-	-	mAcc: **92%**	-	Nine CISs retrieval	Deep learning

Note: The table contents are sorted first by the task column and second by year; mAcc = mean accuracy.

6. Conclusions

This paper provides a detailed review of the current research development in lung CT signs detection, with a focus on the traditional machine learning and deep learning sign research approaches. The sign research method based on traditional machine learning methods is divided into three parts: candidate region segmentation, feature extraction, and feature classification, while the deep learning methods are divided into three parts: classification and image retrieval.

Through comparative examination of existing methodologies, current research on lung CT signatures displays the following characteristics: (1) Compared with earlier research, both machine learning and deep learning approaches have greatly improved the model performance. (2) The deep learning methods can automatically extract deeper features of the image and perform end-to-end supervised training, making it easier to achieve full automation compared to traditional machine learning methods, and the overall detection performance of the model is better than traditional methods, with more classification and image retrieval tasks. (3) The research on sign classification, segmentation, and object detection tasks is unbalanced, with substantial advances in classification tasks, while there is a scarcity of research concentrating on segmentation and object detection tasks. The fundamental explanation for this is presumably the absence of well-annotated sign-oriented datasets.

Future research on lung signs may be conducted from the following viewpoints, based on the characteristics and development trend of present methods:

1. Create sign-oriented datasets. The publicly accessible database LISS, in terms of signs, only comprises 271 case data, which is far from the quantity of data necessary to train deep learning networks. Therefore, building a larger-scale sign-oriented lung CT annotated dataset is vital for the development of lung CT sign recognition, especially for carrying out research on sign identification based on deep learning methods.
2. Relieve the dependency on manually labeled data, a potential strategy has to be utilized: semi-supervised learning. This technique needs to receive more attention. Since enormous success of SSL has been accomplished in the field of natural images, applying current improvements of SSL to medical imaging difficulties looks to be a viable strategy. There is a lack of material focused on semi-supervised CISs detection. It would be a good concept to transfer the semi-supervised approaches in the field of natural images to the field of medical images and to innovate on this basis.
3. Design a sign-based assisted diagnosis system for lung diseases that physicians may utilize to assess symptoms and diagnose lung abnormalities, to encourage in-depth research and development of lung sign detecting tasks using real clinical demands as a reference.

Author Contributions: Conceptualization, H.X. and Y.L.; investigation, Y.L., Y.W. and H.L.; writing—original draft preparation, Y.W.; writing—review and editing, Q.X. and B.J.; funding acquisition, H.X. and Y.L. All authors have read and agreed to the published version of the manuscript.

Funding: This work was supported by the National Natural Science Foundation of China (Grant Nos. 61971078, 51875056), Science and Technology Foundation of Chongqing Education Commission (Grant No. KJQN201901142), Chongqing Natural Science Foundation (Grant No. 2022NSCQ-MSX1902, cstc2020jcyj-msxm2928, 2022NSCQ-MSX1393, 2022NSCQ-BHX2296), General Project (No. E010221003) of the National Cancer Center/National Clinical Research Center for Cancer/Cancer Hospital and Shenzhen Hospital, Chinese Academy of Medical Sciences and Peking Union Medical College.

Institutional Review Board Statement: Not applicable

Informed Consent Statement: Not applicable

Data Availability Statement: Not applicable

Conflicts of Interest: The authors declare no conflicts of interest.

References

1. Sung, H.; Ferlay, J.; Siegel, R.L.; Laversanne, M.; Soerjomataram, I.; Jemal, A.; Bray, F. Global cancer statistics 2020: GLOBOCAN estimates of incidence and mortality worldwide for 36 cancers in 185 countries. *CA Cancer J. Clin.* **2021**, *71*, 209–249. [CrossRef] [PubMed]
2. Kian, W.; Zemel, M.; Levitas, D.; Alguayn, W.; Remilah, A.A.; Rahman, N.A.; Peled, N. Lung cancer screening: A critical appraisal. *Curr. Opin. Oncol.* **2022**, *34*, 36–43. [CrossRef] [PubMed]
3. Hong, B.Y. Diagnostic value of CT for single tuberculosis cavity and canserous cavity. *Chin. J. CT MRI* **2021**, *19*, 139.
4. Xia, X.; Wang, C.J.; Wang, Y. The diagnostic value of deep lobulation and short burrs in cavity lung cancer. *Chin. J. Med. Clin.* **2021**, *21*, 2469–2470.
5. Yu, Y.; Zhang, Y.; Zhang, F.; Fu, Y.C.; Xu, J.R.; Wu, H.W. Value of CT signs in determining the invasiveness of lung adenocarcinoma manifesting as pGGN. *Int. J. Med. Radiol.* **2021**, *43*, 639–643.
6. Armato, S.G., III; McLennan, G.; Bidaut, L.; McNitt-Gray, M.F.; Meyer, C.R.; Reeves, A.P.; Clarke, L.P. The lung image database consortium (LIDC) and image database resource initiative (IDRI): a completed reference database of lung nodules on CT scans. *Med. Phys.* **2011**, *38*, 915–931. [CrossRef]
7. Setio, A.A.A.; Traverso, A.; De Bel, T.; Berens, M.S.; Van Den Bogaard, C.; Cerello, P.; Jacobs, C. Validation, comparison, and combination of algorithms for automatic detection of pulmonary nodules in computed tomography images: The LUNA16 challenge. *Med. Image Anal.* **2017**, *42*, 1–13. [CrossRef]
8. Van Ginneken, B.; Armato, S.G., III; de Hoop, B.; van Amelsvoort-van de Vorst, S.; Duindam, T.; Niemeijer, M.; Prokop, M. Comparing and combining algorithms for computer-aided detection of pulmonary nodules in computed tomography scans: The ANODE09 study. *Med. Image Anal.* **2010**, *14*, 707–722. [CrossRef]
9. Dolejsi, M.; Kybic, J.; Polovincak, M.; Tuma, S. The lung time: Annotated lung nodule dataset and nodule detection framework. In Proceedings of the Medical Imaging2009: Computer-Aided Diagnosis, Lake Buena Vista, FL, USA, 10–12 February 2009; pp. 538–545.
10. Depeursinge, A.; Vargas, A.; Platon, A.; Geissbuhler, A.; Poletti, P.A.; Müller, H. Building a reference multimedia database for interstitial lung diseases. *Comput. Med. Imaging Graph.* **2012**, *36*, 227–238. [CrossRef]
11. Han, G.; Liu, X.; Han, F.; Santika, I.N.T.; Zhao, Y.; Zhao, X.; Zhou, C. The LISS—A public database of common imaging signs of lung diseases for computer-aided detection and diagnosis research and medical education. *IEEE Trans. Biomed. Eng.* **2014**, *62*, 648–656. [CrossRef]
12. Guo, K.; Liu, X.; Soomro, N.Q.; Liu, Y. A novel 2D ground-glass opacity detection method through local-to-global multilevel thresholding for segmentation and minimum bayes risk learning for classification. *J. Med. Imaging Health Inform.* **2016**, *6*, 1193–1201. [CrossRef]
13. Huang, S.; Liu, X.; Han, G.; Zhao, X.; Zhao, Y.; Zhou, C. 3D GGO candidate extraction in lung CT images using multi-level thresholding on supervoxels. In Proceedings of the Medical Imaging: Computer-Aided Diagnosis, Houston, TX, USA, 12–15 February 2018; p. 1057533.
14. Dhara, A.K.; Mukhopadhyay, S.; Saha, P.; Garg, M.; Khandelwal, N. Differential geometry-based techniques for characterization of boundary roughness of pulmonary nodules in CT images. *Int. J. Comput. Assist. Radiol. Surg.* **2016**, *11*, 337–349. [CrossRef] [PubMed]
15. Cui, W.; Wang, Y. A Lung Calcification Detection Method through Improved Two-dimensional OTSU and the combined features. In Proceedings of the IEEE International Conference on Artificial Intelligence and Computer Applications, Dalian, China, 29–31 March 2019; pp. 369–373.
16. Xiao, H.G.; Ran, Z.Q.; Huang, J.F.; Ren, H.J.; Liu, C.; Zhang, B.L.; Zhang, B.L.; Dang, J. Research progress in lung parenchyma segmentation based on computed tomography. *J. Biomed. Eng.* **2021**, *38*, 379–386.
17. Farheen, F.; Shamil, M.S.; Ibtehaz, N.; Rahman, M.S. Revisiting segmentation of lung tumors from CT images. *Comput. Biol. Med.* **2022**, *144*, 105385. [CrossRef]
18. Zhao, X.; Zhang, P.; Song, F.; Fan, G.; Sun, Y.; Wang, Y.; Tian, Z.; Zhang, L.; Zhang, G. D2A U-Net: Automatic segmentation of COVID-19 CT slices based on dual attention and hybrid dilated convolution. *Comput. Biol. Med.* **2021**, *135*, 104526. [CrossRef]
19. Fan, D.P.; Zhou, T.; Ji, G.P.; Zhou, Y.; Chen, G.; Fu, H.; Shao, L. Inf-net: Automatic covid-19 lung infection segmentation from ct images. *IEEE Trans. Med. Imaging* **2020**, *39*, 2626–2637. [CrossRef]
20. Zheng, B.; Liu, Y.; Zhu, Y.; Yu, F.; Jiang, T.; Yang, D.; Xu, T. MSD-Net: Multi-scale discriminative network for COVID-19 lung infection segmentation on CT. *IEEE Access* **2020**, *8*, 185786–185795. [CrossRef]
21. Song, L.; Liu, X.; Ma, L.; Zhou, C.; Zhao, X.; Zhao, Y. Using HOG-LBP features and MMP learning to recognize imaging signs of lung lesions. In Proceedings of the 25th IEEE International Symposium on Computer-Based Medical Systems (CBMS), Rome, Italy, 20–22 June 2012; pp. 1–4.
22. Kashif, M.; Raja, G.; Shaukat, F. An Efficient Content-Based Image Retrieval System for the Diagnosis of Lung Diseases. *J. Digit. Imaging* **2020**, *33*, 971–987. [CrossRef]
23. Ma, L.; Liu, X.; Gao, Y.; Zhao, Y.; Zhao, X.; Zhou, C. A new method of content based medical image retrieval and its applications to CT imaging sign retrieval. *J. Biomed. Inform.* **2017**, *66*, 148–158. [CrossRef]

24. Liu, X.; Ma, L.; Song, L.; Zhao, Y.; Zhao, X.; Zhou, C. Recognizing common CT imaging signs of lung diseases through a new feature selection method based on Fisher criterion and genetic optimization. *IEEE J. Biomed. Health Inform.* **2014**, *19*, 635–647. [CrossRef]
25. Sun, S.S.; Ren, H.Z.; Kang, Y.; Zhao, H. Pulmonary nodules detection based on genetic algorithm and support vector machine. *J. Syst. Simul.* **2011**, *23*, 497–501.
26. Ma, L.; Liu, X.; Fei, B. Learning with distribution of optimized features for recognizing common CT imaging signs of lung diseases. *Phys. Med. Biol.* **2016**, *62*, 612. [CrossRef] [PubMed]
27. Ma, L.; Liu, X.; Song, L.; Zhao, C.; Zhao, X.; Zhou, Y. A new classifier fusion method based on historical and on-line classification reliability for recognizing common CT imaging signs of lung diseases. *Comput. Med. Imaging Graph.* **2015**, *40*, 39–48. [CrossRef]
28. Han, G.; Liu, X.; Zhang, H.; Zheng, G.; Liu, W. Hybrid resampling and multi-feature fusion for automatic recognition of cavity imaging sign in lung ct. *Future Gener. Comput. Syst.* **2019**, *99*, 558–570. [CrossRef]
29. Shen, R.; Cheng, I.; Basu, A. A hybrid knowledge-guided detection technique for screening of infectious pulmonary tuberculosis from chest radiographs. *IEEE Trans. Biomed. Eng.* **2010**, *57*, 2646–2656. [CrossRef] [PubMed]
30. Xu, T.; Cheng, I.; Long, R.; Mandal, M. Novel coarse-to-fine dual scale technique for tuberculosis cavity detection in chest radiographs. *Eurasip J. Image Video Process.* **2013**, *2013*, 3. [CrossRef]
31. Han, G.; Liu, X.; Zheng, G.; Wang, M.; Huang, S. Automatic recognition of 3D GGO CT imaging signs through the fusion of hybrid resampling and layer-wise fine-tuning CNNs. *Med. Biol. Eng. Comput.* **2018**, *56*, 2201–2212. [CrossRef]
32. Shin, H.C.; Roth, H.R.; Gao, M.; Lu, L.; Xu, Z.; Nogues, I.; Summers, R.M. Deep convolutional neural networks for computer-aided detection: CNN architectures, dataset characteristics and transfer learning. *IEEE Trans. Med. Imaging* **2016**, *35*, 1285–1298. [CrossRef]
33. Song, Y.; Cai, W.; Huang, H.; Zhou, Y.; Feng, D.D.; Wang, Y.; Chen, M. Large margin local estimate with applications to medical image classification. *IEEE Trans. Med. Imaging* **2015**, *34*, 1362–1377. [CrossRef]
34. Zheng, G.; Han, G.; Soomro, N.Q. An inception module CNN classifiers fusion method on pulmonary nodule diagnosis by signs. *Tsinghua Sci. Technol.* **2019**, *25*, 368–383. [CrossRef]
35. Frid-Adar, M.; Klang, E.; Amitai, M.; Goldberger, J.; Greenspan, H. Synthetic data augmentation using GAN for improved liver lesion classification. In Proceedings of the15th IEEE International Symposium on Biomedical Imaging, Washington, DC, USA, 4–7 April 2018; pp. 289–293.
36. Zhuang, F.Z.; Qi, Z.Y.; Duan, K.Y.; Xi, D.B.; Zhu, Y.C.; Zhu, H.S.; Xiong, H.; He, Q. A comprehensive survey on transfer learning. *Proc. IEEE* **2021**, *109*, 43–76. [CrossRef]
37. Gui, J.; Sun, Z.; Wen, Y.; Tao, D.; Ye, J. A review on generative adversarial networks: Algorithms, theory, and applications. *IEEE Trans. Knowl. Data Eng.* **2021**, 1. [CrossRef]
38. He, G. Lung ct imaging sign classification through deep learning on small data. *arXiv* **2019**, arXiv:1903.00183.
39. Zheng, G.; Han, G.; Soomro, N.Q.; Ma, L.; Zhang, F.; Zhao, Y.; Zhou, C. A novel computer-aided diagnosis scheme on small annotated set: G2C-CAD. *BioMed Res. Int.* **2019**, *2019*, 6425963. [CrossRef]
40. Zhao, J.J.; Pan, L.; Zhao, P.F.; Tang, X.X. Medical sign recognition of lung nodules based on image retrieval with semantic features and supervised hashing. *J. Comput. Sci. Technol.* **2017**, *32*, 457–469. [CrossRef]
41. Zhang, Y.N.; Zhao, L.J.; Wu, W.; Geng, X.; Hou, G.J. Alternate optimization of 3D pulmonary nodules retrieval based on medical signs. *J. Taiyuan Univ. Technol.* **2022**, *53*, 8.
42. Nora, Y.; Ayman, Al.; Sahar, M.; Hany, H. An Intelligent CBMIR System for Detection and Localization of Lung Diseases. *Int. J. Adv. Res.* **2021**, *9*, 651–660.
43. Ma, L.; Liu, X.; Fei, B. A multi-level similarity measure for the retrieval of the common CT imaging signs of lung diseases. *Med. Biol. Eng. Comput.* **2020**, *58*, 1015–1029. [CrossRef]